09 May 1984, 9:00 am - 12:00 pm

Post-Earthquake Failure of a Tailings Dam Due to Liquefaction of Pond Deposit

Kenji Ishihara
University of Tokyo, Japan

Post-Earthquake Failure of a Tailings Dam Due to Liquefaction of the Pond Deposit

Kenji Ishihara
Department of Civil Engineering, University of Tokyo

ABSTRACT At the time of the Izu-Ohshima-Kinkai earthquake of January 15, 1978 in Japan, two dams retaining tailings from Mochikoshi gold mine failed, leading to a release of a large volume of tailings. One of the dams, No.1 dike, collapsed almost simultaneously with the shaking of the main shock, but another dam, No.2 dike, failed about 24 hours later at a time when there was no shaking. The failure of the No.1 dike is known to have been triggered by the liquefaction which developed in the tailings deposit in the impoundment pond. The cause of the failure in the No.2 dike has not, however, been studied and left open to question. To provide a basis to answer this question, an attempt was made to analyze outward movement of phreatic surface within the dike fills which is motivated by an increase in pore water pressure due to liquefaction developing in the pond deposit behind the retaining dike. It was shown that the phreatic surface could move up to a level near the downstream surface by the time the failure of the dike took place. At each stage of the phreatic surface movement slope stability analysis was performed using the conventional method and factors of safety were calculated. Results of the analyses showed that the factor of safety drops approximately to unity at the stage when the phreatic surface reaches a location in proximity to the surface of the slope. The period of time elapsed for the phreatic surface to reach the near-surface location was also computed and shown to be nearly coincident with the time period between when the earthquake occurred and when the failure actually took place in the No.2 dike.

INTRODUCTION

The tailings deposits in the impoundment ponds are usually soft, loose and permanently saturated. Consequently they will tend to liquefy at an early stage of major earthquakes, applying an increased horizontal load on the dam retaining the tailings. Therefore, the occurrence of liquefaction could be a potential hazard that can lead to catastrophic failure of the tailings impoundment dams. In fact, several cases of such dam incidents have been reported recently. Failures of the Barahona dam, Chile, in 1928 (Aguero, 1929), El Coble dam, Chile, in 1965 (Dobry and Alvarez, 1967) and Mochikoshi dam, Japan in 1978 (Marcuson, 1979: Ohkusa and Anma, 1980) are typical examples of failures of the tailings dams.

All of these documented cases describe failures of dams as having taken place almost simultaneously with or immediately after the shaking of earthquakes. However, in the case of the incident at Mochikoshi tailings dams in 1978, Japan, while the No.1 dam failed at the same time as the main shaking, the breach of the No.2 dike took place about one day after the main shock of the earthquake at a quiet time without any tremor. According to the report (1979) issued by the Investigation Committee, the cause of the breach at No.1 dike is attributed to the occurrence of liquefaction in the disposal pond and consequent loss of stability of the retaining dam. With respect to the failure of No.2 dike, no clear-cut interpretation is presented for mechanism triggering the breach, probably because the problem was for from conclusive.

In view of the context as above, an attempt has been made to develop a concept and procedure enabling a mechanism of the delayed failure to be clarified for the incident of the No.2 dike at Mochikoshi. In the following pages, the consequence of this study will be presented, together with the general outline concerning the 1978 earthquake, construction and operation of the tailings disposal pond and results of soil investigations. The general information as above on the Mochikoshi tailings dam was quoted from the report of the Investigation Committee.

IZU-OHSHIMA-KINKAI EARTHQUAKE OF 1978

On January 14, 1978, a destructive earthquake of Magnitude 7.0 shock the southeastern area of Izu Peninsula which is located about 120 km southwest of Tokyo, Japan (Fig. 1). The epicenter of the main shock was located about 15 km off the east coast of the peninsula, midway between the peninsula and Ohshima Island as shown in Fig. 2. The main shock was followed by a series of aftershocks lasting for a week with their epicenters moving gradually in a westerly direction. The epicenters of the aftershocks with a magnitude greater than M = 4.0 are also indicated in Fig. 2 by solid circles. The largest aftershock was a pair of shakings that took place at 7:30 a.m. and 7:36 a.m. on January 15, 1978 with their epicenters located approximately in the middle of the Izu-Peninsula in proximity to the Mochikoshi tailings dam site. Most of the shocks are presumed to have had a focal depth of about 10 km. The

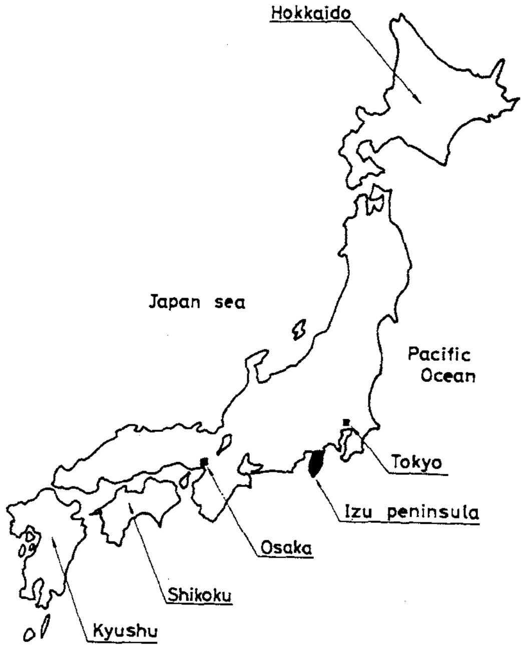

Fig. 1. Location of Izu Peninsula

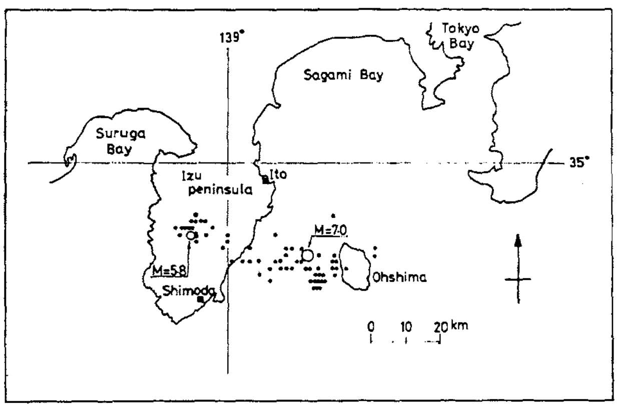

Fig. 2. Locations of the main shock and aftershocks of Izu- Ohshima-Kinkai earthquake

strong shaking motion produced by the earthquake was recorded at several stations, but all of them were obtained outside the area of highest intensity shaking. A survey of the overturning of tombstones in many cemeteries near the epicentral region disclosed an approximate picture of distribution of shaking intensity. Fig. 3 shows contour lines of equal maximum horizontal acceleration thus established (Ohashi et. al, 1978). It may be seen that at Mochikoshi site the acceleration is estimated to be approximately 250 gal on the ground surface. A more detailed account on the earthquake and damage feature is given in a previous paper by Ishihara and Nagao (1983).

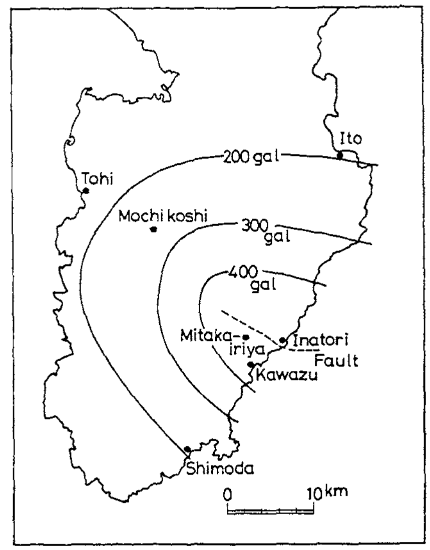

Fig. 3. Contours of equal shaking intensity in terms of estimated maximum horizontal accelerations

CONSTRUCTION OF TAILINGS CONTAINMENT DIKES

The Hozukizawa disposal pond at Mochikoshi was constructed on a bowl-shaped depression on top of a mountain shown in Fig. 4 by sealing off the periphery by three dikes. The plan view of the pond is shown in Fig. 5. The site consists of weathered deposit of cobble-containing tuffs which were transported by a series of eruptions of volcanos in the mountian ridge in its neighborhood. At the initial stage of construction strongly weathered surface portion was stripped off and less weathered tuff formation was exposed in a saw-teeth shape to provide rough surface for the foundation of the overlying starter dam. The starter dam was constructed in 1964 by placing local soils of volcanic origin by means of bulldozers. During the construction operation the passages of bulldozers helped compact the soils to a desired density. In order to provide drainage for water emerging from nearby springs, a system of drainage consuit was installed at the bottom of the starter dam. However, because of a relatively high degree of permeability provided by the original mountain deposit, no drainage system was installed over the bottom of the pond for draining excess water resulting from consolidation of tailings sludge.

The mine milling operation to extract gold was conducted in the processing plants beside the Mochikoshi river (Fig. 4). The tailings produced there in slurry had been pumped through pipes through a height of 600 m up to the disposal pond located on top of the mountain. The pupmed-up slurry was delivered either to the site of No.1 or No.2 dike and discharged towards the pond from three pipes at each dike site. The dike was successively raised by placing the local volcanic soils at a rate of approximately 2 m per year by what is called upstream filling method.

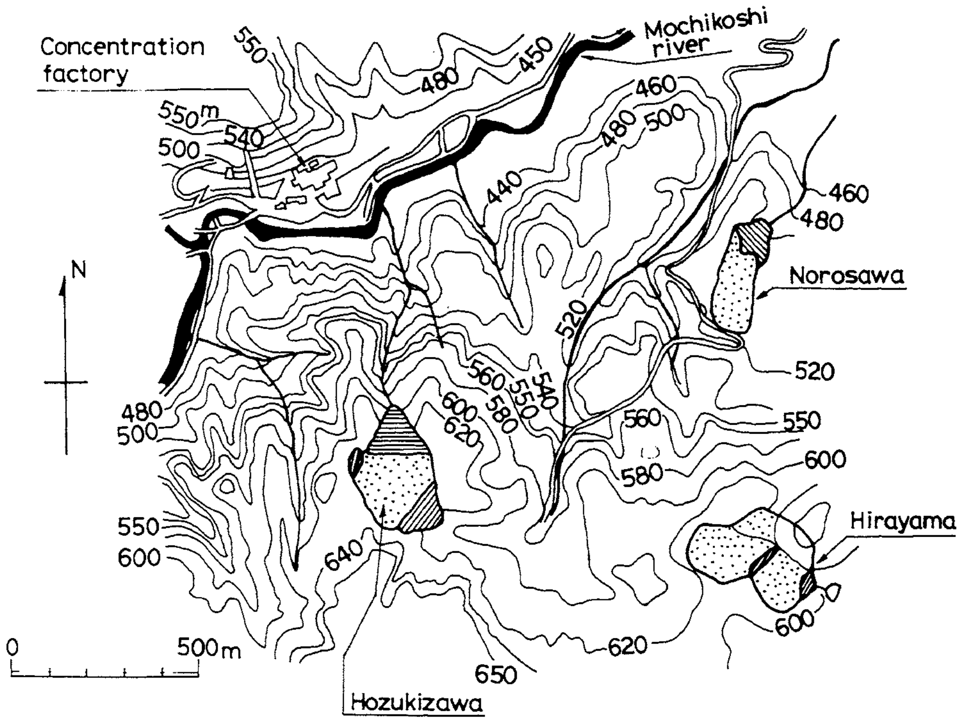

Fig. 4. Location of Hozukizawa Tailings ponds

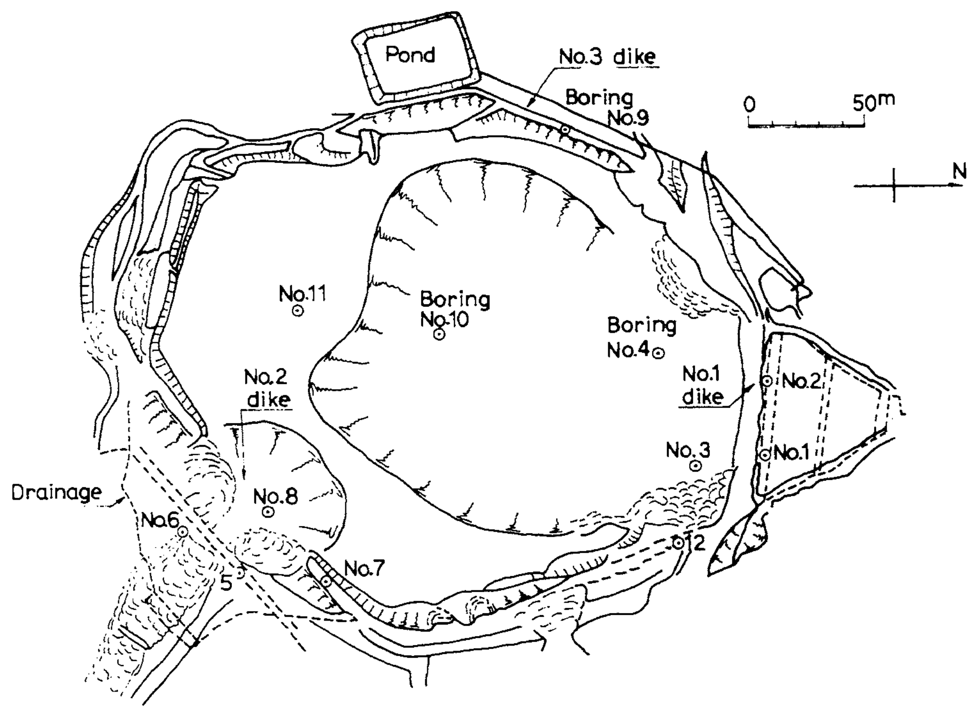

Fig. 5. Plan of the Hozukizawa disposal pond at Mochikoshi

DAMAGE TO TAILINGS DAMS

1. Failure of No.1 Dike

The failure of No.1 Dike was triggered by the main shock of the Izu-Ohshima-Kinkai earthquake. The feature of the collapse is demonstrated in the cross section shown in Fig. 6. The biggest next biggest with a magnitude of 5.4 at 7:36 a.m. After these shocks around 8:30 a.m., a surveillant found five to six cracks developing on the downslope face in parallel with the axis of the dike. These cracks were reportedly 1 to 3 meter long with openings about 5 mm wide. At a later time around 9:30 p.m., another surveillant discovered a longitudinal crack, opening 5 m long and 5 cm wide in the middle of the

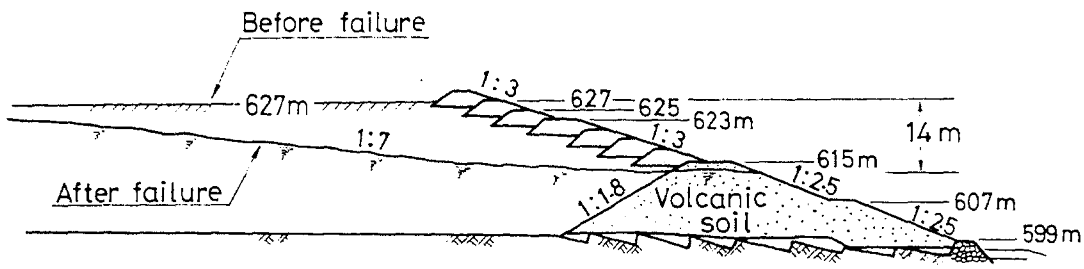

Fig. 6. Cross-section through embankment of No.1 dike

dike 28 m high and 73 m wide at crest level collapsed almost at the same time as the major shaking of the earthquake. A quardian of the pond who happened to be stationed at a house on the left bank came out immediately upon perceiving an unusually high shaking and watched the terrific moment of disaster. According to his account, within a matter of 10 seconds after the main shock, the frontal wall of the dike swelled and the breach took place at the upper part in proximity to the left abutment, followed by a huge mass of slime rushing down the valley with a dreadful wham whereby mowing trees and scoring the bottom of the valley. When the rushing slime came to the junction with the Mochikoshi river, the slime hit the flank of masonry walls, jumping up about 10 m high on the lift bank of the river channel and deposited to about 30 cm thickness over the road beside the channel. The slime flowed down the Mochikoshi river sedimenting in the river bed to a thickness of 1.0 to 1.9 m through the distance of about 800 m from the point of confluence. The flowing slime further travelled into the Kano river and contaminated the river through a distance of about 10 km down to the mouth of the river.

The top portion of the No.1 dike failed totally through a height of 14 m from the top level of impoundment down to the elevation of the starter dam, as illustrated in Fig. 6. A total volume of 80,000 m^3 was released as a result of the dike failure, of which 60,000 m^3 was the tailings and 20,000 m^3 the dike-forming volcanic ashes.

2. Failure of No.2 Dike

As described in the foregoing, a series of medium-sized earthquakes rocked the central part of the Izu peninsula from early morning to noon time on the day of January 15, 1978. The biggest aftershocks occurred at 7:31 a.m. with a magnitude 5.8, followed immediately by the downstream slope of the No.2 dike.

At about 1:00 p.m. on that day, a caretaker standing on the opposite side of the No.2 dike happened to notice a gradual sinking of the central part of the dam. While running to the dam site, he watched the dam failing suddenly through a crest width of about 20 m leading to a release of the impounded tailings sludge. Later on the breach was enlarged to a crest length of 65 m, generating a number of cracks over the sloughing surface. A total volume of 3,000 m^3 consisting of 2,000 m^3 of tailings slime and 1,000 m^3 of dike material flowed down the valley to a distance of about 240 m. The feature of the collapse is shown in Fig. 7. The portion of the five-step dike additions above the starter dam was taken away, as shown in Fig. 7. The plan view of this slide is shown in Fig. 5.

SITE INVESTIGATIONS AND SOIL TESTS

After the failure of the dikes, in-situ investigation on soils and ground water conditions was carried out, together with appropriate laboratory tests on tailings and on soil samples recovered from the inflicted site.

1. Soil Profiles and Standard Penetration Tests

Borings were made at 12 locations in and near the disposal pond, as indicated in Fig. 5. The boring logs in the vicinity of the No.1 dike are shown in Figs. 8 through 10 and those conducted near the No.2 dike are demonstrated in Figs. 11 through 12. The log of Boring No.2 drilled from the exposed failure surface reveals the presence of a thick layer of fill composed of weathered volcanic ashes underlying the deposit of the tailings slime. This fill is the

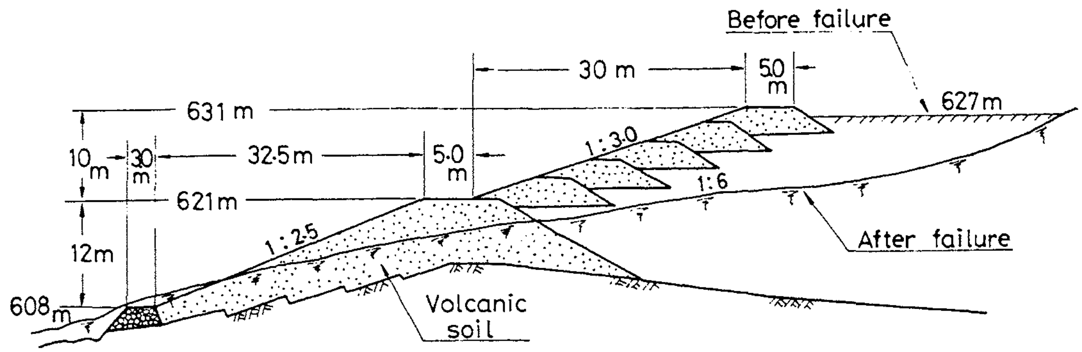

Fig. 7. Cross-section through embankment of No.2 dike

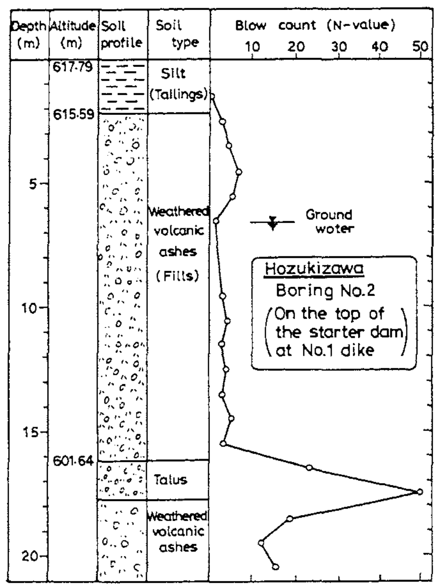

Fig. 8. Soil profile at No.1 dike (From report of the investigation committee)

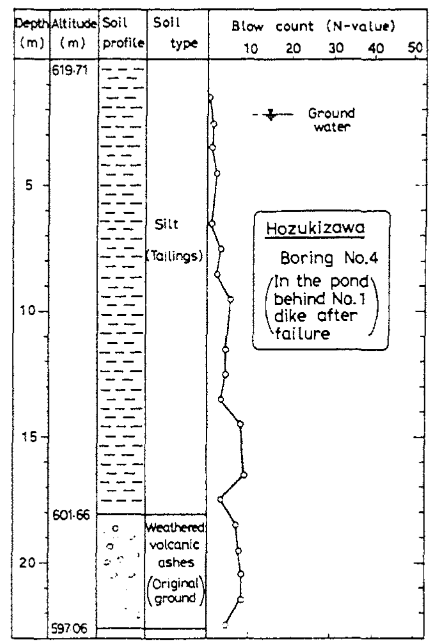

Fig. 9. Soil profile behind No.1 dike (From report of the investigation committee)

main body of the starter dam. It may been seen in Fig. 8 that the fill had a blown count value of 3 to 7 in the standard penetration test. The log of Boring 4 conducted in the interior part of the pond indicates that there exists a thick layer of tailings sludge down to a depth of 18 m underlaid by an original deposit in the mountain. The result of the standard penetration test indicates blow count values on the order of 1 to 2 near the surface but somewhat larger values of 4 to 9 in the lower half portion of the sludge deposit. The progression of consolidation with drainage towards the permeable bed soils may have stiffen the slime deposit near the bottom of the disposal pond. Near the surface which coincides with the failure plane, the penetration rod sank by its self-weight to a depth of 2 m without any hammer blow. The presence of the extremely soft layer must have acrued as a result of liquefaction developed to this elevation during the quake. The log of Boring No. 10 drilled in the center of the pond indicates a complete soil profile from the pre-earthquake surface level not stripped off by the failure. The blow count value is equal to zero down to a depth of 15 m, whereupon it increases to a value between 3 and 6 near the bottom of the slime deposit. Underneath the slime layer these exists the original deposit of the mountain consisting mainly of weathered volcanic ashes. The fact that there is little resistance to penetration down to the depth of 15 m does not appear to have ever been so, but seems to have been caused by the occurrence of liquefaction due to the earthquake.

The log of Boring No.8 obtained from the failure surface at No.2 dike is demonstrated in Fig. 11, where it may be seen that the tailings slime deposit was probably remolded down to an elevation of 614.50 m as a result of liquefaction

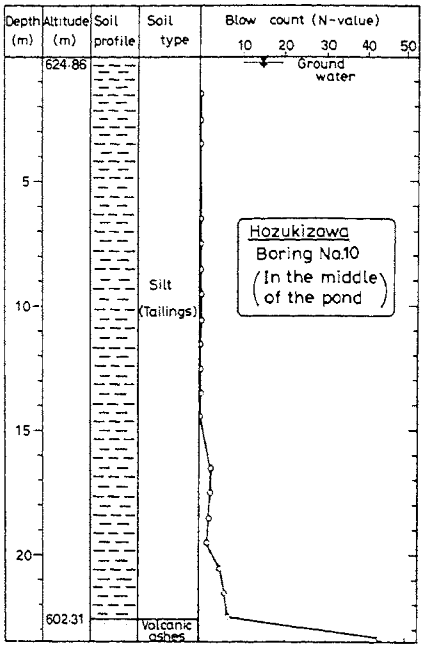

Fig. 10. Soil profile in the middle of Hozukizawa pond (From report of the investigation committee)

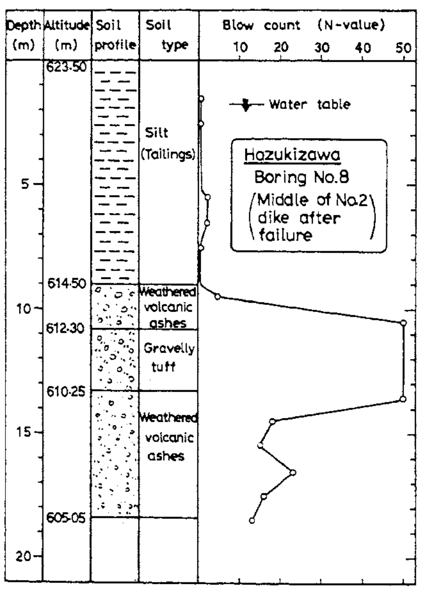

Fig. 11. Soil profile at No.2 dike (From report of the investigation committee)

during the earthquake. The layers of deposit underlying the tailings slime are those of original mountain deposits at this site, as can be seen from the location of this boring site shown in Fig. 5. The soil profile data at Boring No. 5 shown in Fig. 12 was obtained from the top of the starter dam and accordingly it misses the

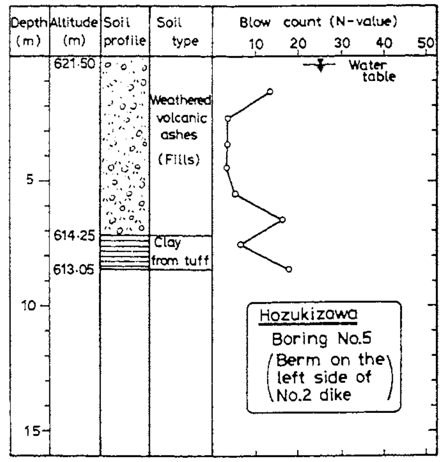

Fig. 12. Soil profile at No. 2 dike (From report of the investigation committee)

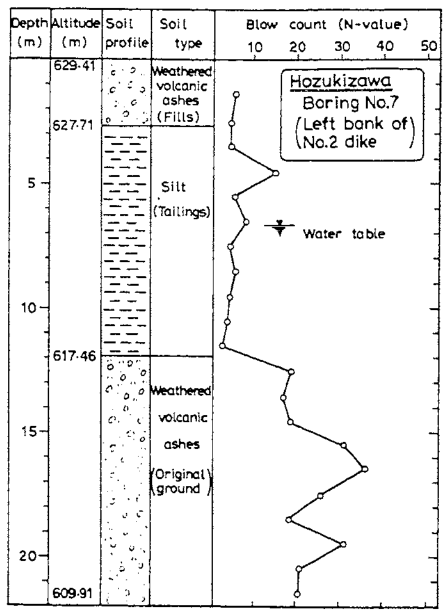

Fig. 13. Soil profile at No.2 dike (From report of the investigation committee)

portion of the slime deposit. The standard penetration test results show a blow count value of 4 to 5 for the bulldozer-rolled fill of the starter dam. Still another log of Boring 7 obtained from the top of an intact portion of the No.2 dike indicates, as shown in Fig. 13, that the bulldozer-rolled fills constructed by the stepwise top additions had a blow count value of approximately 5.

Reviews of the boring logs as above indicate generally that the slime deposit near the bottom of the pond had been consolidated having a blow count value of 3 to 7, whereas the slime near the failure surface was soft having almost zero blow count value probably because of the remolding due to liquefaction. The containment dikes constructed by additions of several steps of bulldozer-rolled fills had a blow count value of approximately 5 and a similar degree of penetration resistance was observed for the portion of the starter dam.

2. Phreatic Level and Pearmeability Studies.

Observation of water level in piezometer pipes had been underway in the No.1 dike for surveillance purposes prior to the earthquake. The water level along the slope was relatively stationary and a set of surveillance results made latest to the time of the earthquake provided levels of phreatic surface at several locations on the downstream slope which were consistently about 3 m below the slope surface. A straight line parallel to the slope surface was thus regarded as representing the phreatic line existing in the No.1 dam at the time of the earthquake. For the No.2 dike there is no surveillance data identifying an exact location of the phreatic surface. However, in view of almost similar conditions in every respect, it may well be conceived that the phreatic surface in No.2 dike was also about 3 m below the slope surface.

Permeability studies were also conducted both in-situ and in the laboratory. The permeability coefficient obtained from the in-situ grouting method indicated a value on the order of 10^{-4} cm/sec for the bulldozer-rolled dike material and 10^{-3} cm/sec for the original bed rock composed of weathered tuffs. The permeability coefficient of the tailings deposit was estimated to be approximately 7×10^{-4} cm/sec in the horizontal direction , but because of a highly stratified nature of the sediment, the permeability in the vertical direction is supposed to have been as small as one thousandth to one hundredth.

3. Index Properties and Strength Tests

Tailings Materials

Over the surface of the disposal pond on the west side of the No.2 dike, a number of sand volcanos were observed following the earthquake. One of the biggest volcanos about 2 m in diameter of sand spread was carefully excavated to a depth of about 50 cm. The cross-section through the sand volcano thus obtained is shown in Fig. 14, where it can be seen that sand-containing silt (sandy silt) and fine-grained material (silt) are deposited, one on top of the other, in thin layers 3 to 7 cm in thickness. Two batches of samples were recovered seperately each from the portion of coarse-grained and fine-grained layers. The grain size distribution curves for each portion are shown in Fig. 15. Also shown in Fig. 15 are two grain size distribution curves for the blended samples obtained by a shovel in block. It is to be noted that there is an upper limit in grain size which is 0.3 mm. This is the maximum grain size specified in the grinding process of the ore. Fig. 15 also shows that the grain size distribution curves for two blended samples lie within the range bounded by those of the silty sand and silt. Void ratio of the tailings was 0.98 and 1.00, and the specific

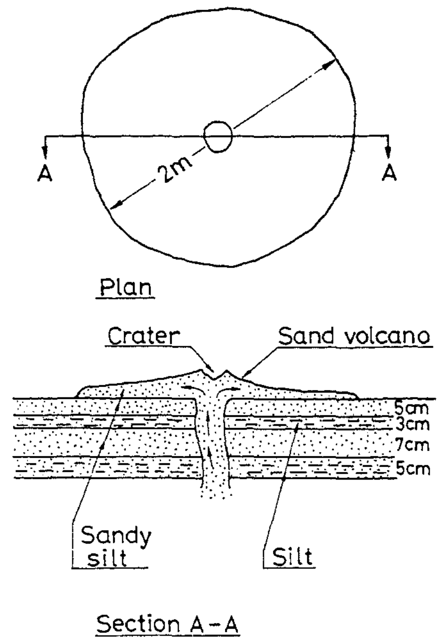

Fig. 14. Cross section of a sand volcano formed on the surface of the disposal pond

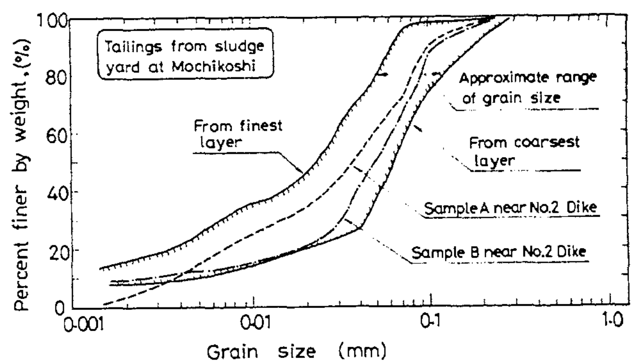

Fig. 15 Grain size distribution curves of tailings materials from Mochikoshi mine

gravity was 2.72 and 2.74, respectively, for the sandy silt and silt portion. Plasticity index was 10 for the silt but the sandy silt was identified as non-plastic. The index properties of the tailings are summarized Table 1.

Several series of cyclic as well as static strength tests were conducted on both disturbed and undisturbed samples of the tailings sludge by using the triaxial test apparatus. These triaxial tests were run under consolodated-undrained conditions with pore water pressure measurements. Results of cyclic tests on disturbed specimens are described in a previous publication (Ishihara et al, 1980). Undisturbed samples of the tailings were secured by means of

Table 1. Physical properties of tailings

Items	Notations	Sandy silt	Silt
Specific Gravity	Gs	2.72	2.74
Liquid Limit	W_L (%)	27	31
Plastic Limit	W_P (%)	Non-plastic	21
Plasticity Index	PI	Non-plastic	10
In-situ water contant	ω (%)	36	37
In-situ void ratio	e	0.98	1.00
In-situ consolidation coefficient	C_v (cm^2/min)	——	0.1~0.8 load(0~0.6 kg/cm^2)
In-situ volume compressibility	m_v (cm^2/kg)	——	5.5~22x10^{-2} load(0~0.6 kg/cm^2)

thin-wall tubes. The samples encased in the tubes were once frozen to minimize the disturbance during transportation. The samples were thawed in the laboratory and tested with an appropriate back pressure to ensure full saturation of the specimen. Results of the static triaxial shear tests indicated zero cohesion component ($C' = 0$) and an angle of internal friction, ϕ', varying between 30° and 39°, in terms of the effective stress representation. The angle of internal friction for the Mochikoshi tailings material was shown to be expressed approximately by

$$\tan\phi' = \frac{0.7}{e} \qquad \cdots\cdots\cdots(1)$$

where e denotes the void ratio. One of the results of the cyclic triaxial shear tests is shown in Fig. 16 in terms of a relationship

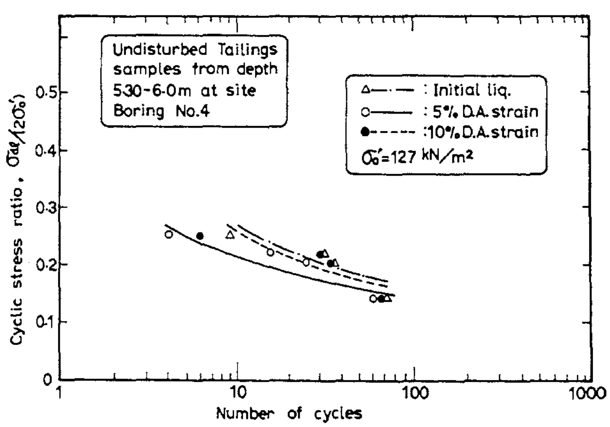

Fig. 16. Cyclic stress ratio versus number of cycles for undisturbed tailings samples from the pond (From report of the investigation committee)

between the cyclic stress ratio, $\sigma_{d\ell}/2(\sigma_0')$ versus the number of cycles required to produce 5 % double-amplitude axial strain in the test specimen, where $\sigma_{d\ell}$ denotes the amplitude of cyclic axial stress and σ_0' is the initial confining pressure. Fig. 16 shows that the cyclic stress ratio causing 5 % double-amplitude axial strain in 20 cycles is on the order of 0.2. The results of the tests on other samples from different sampling sites and from different depths showed more or less similar values of cyclic strength to those shown in Fig. 16. Scrutiny of all the test results showed that the cyclic strength of the Mochikoshi tailings may as well be represented by an empirical formula which is promulgated in the Japanese Design Code for tailings dams (Ishihara et al, 1981). According to the code, the cyclic stress ratio causing 5 % double-amplitude strain in 20 cycles of load application, R_ℓ, is expressed as,

$$R_\ell = 0.088\sqrt{\frac{N}{\sigma_v'+0.7}} + 0.085\log_{10}\left(\frac{0.50}{D_{50}}\right) \qquad \cdots(2)$$

where N is the blow count value in the standard penetration test, and σ_v' is the effective overburden pressure in terms of kg/cm^2.

Dike Materials

The dikes were constructed of a mixture of the weathered tuffs and volcanic ashes covering widespread area of the mountains in the vicinity. The material is a potpourri of gravel, sand and silt, as visualized from the wide range of the grain size distribution curve shown in Fig. 17. Both index property and strength tests were

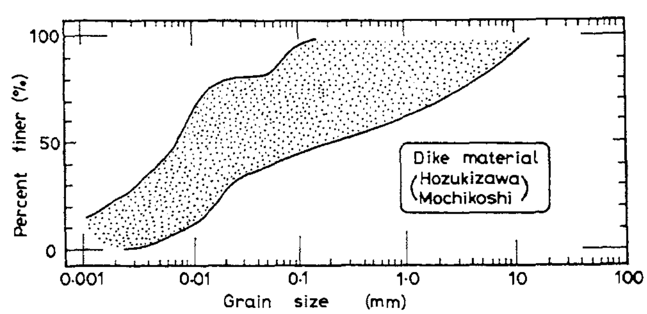

Fig. 17. Distribution of grain sizes in the dikes (From report of the investigation committee)

performed on undisturbed samples secured in chunk near the surface and also on samples recovered in thin-walled tubes from bored holes. Wet unit weight, γ, of the soil ranged between 14 and 19 kN/m^3, natural water content, ω, was 30 to 60 % and void ratio was 1.1 to 2.6. The permeability coefficient of the soil was shown to be approximately on the order of 10^{-4}cm/sec.

With respect to the strength, the consolidated-undrained triaxial shear tests on undisturbed samples trimmed from blocks indicated a cohesion of about $C' = 25$ kN/m^2 and an average angle of internal friction of $\phi' = 35°$. For the dike material, the cyclic triaxial test was not performed.

STABILITY ANALYSES DURING THE EARTHQUAKE

1. Analysis of Liquefaction

Following the earthquake a number of sand volcanos were observed on the intact part of the pond surface which was not disrupted by the flow slide. Also, in view of the surprisingly huge volume of the tailings involved in the flow slide, it was suspected that occurrence of liquefaction might have been responsible for touching off a slide movement of such huge quantity of soil. In view of this, the Investigation Committee made a detailed analysis on the likelihood of liquefaction occurring in the tailings deposit on the basis of the laboratory test results. A detailed study was also performed for assessing the input motion to be incorporated in the response analyses at this site. The maximum horizontal acceleration at the base rock was estimated to have been on the order of 90 gal during the shaking due to the main shock. Seismic response analyses were conducted for different soil profiles in the pond by using the one-dimensional wave propagation theory. The results of the analyses indicated that the maximum horizontal acceleration at the surface level of the disposal pond might have probably been in the range of 150 and 250 gal. The analysis of liquefaction was then made by comparing the seismically induced shear stress to the magnitude of shear stress required to cause failure in the corresponding loading conditions. The results of such analyses indicated that the liquefaction could indeed occur and it could extend down to a depth of approximately 7 m from the surface of the disposal pond.

2. Pseudo-Static Stability Analyses

By incorporating different values of seismic coefficient varying between 0.15 and 0.25, slope stability analyses were made for a circular slip surface representing the actual sliding planes shown in Figs. 6 and 7. The factor of safely against sliding was calculated using the following formula,

$$F = \frac{\Sigma\left[(W\cos\alpha - k_H W\sin\alpha - U\cdot\ell)\tan\phi' + C'\cdot\ell\right]}{\Sigma(W\sin\alpha + k_H W\cos\alpha)} \quad \cdots (3)$$

were w denotes the weight of saturated soil in each sliced element, u is the excess pore water pressure, k_H is the seismic coefficient, α is the angle of inclination of slip plane at the bottom of each slice and ℓ denotes the length of the slip plane at the bottom of each element. The notations are illustrated in Fig. 18.

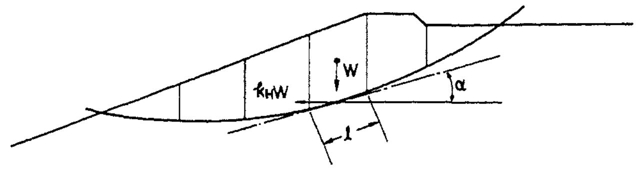

Fig. 18. Division into sliced elements for the stability analysis

Analysis for No.1 dike

The stability analysis was made by the Investigation Committee (1979) for a cross section of the dike having soil properties shown in Fig. 19. The result of the stability analysis showed that for the static condition prior to the earthquake, the factor of safely was 2.32 for No.1 dike. In the seismic loading condition, two cases were considered. In the first case, no excess pore water pressure was allowed for in the analysis and the magnitude of seismic coefficient necessary to bring the computed factor of safely to unity was shown to be as large as 0.3. Then, in the second case some appropriately assessed value of excess pore water pressure due to the seismic shaking was taken into account in the stability computation by Eq.(3). It was found that the seismic coefficient of 0.17 was large enough to bring down the factor of safety to unity from the initial value of 2.32.

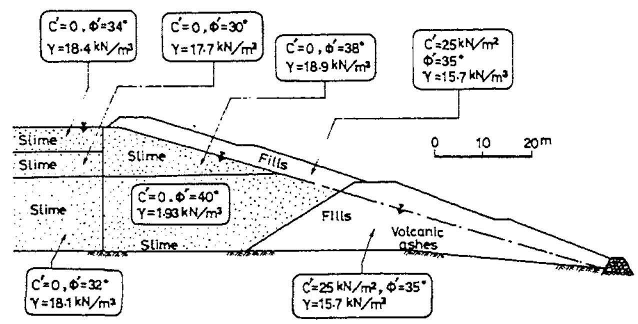

Fig. 19. Cross section of No.1 dike with soil properties used in the stability analysis

Analysis for No.2 dike

The stability analysis for the static loading prior to the earthquake was made by the Investigation Committee (1979) for a cross section of the dike having soil properties shown in Fig. 20. The result of analysis indicated a factor of safety of 2.75. In the case of seismic loading conditions, the seismic coefficient value as much as 0.4 was shown to be needed to bring the computed factor of safety to unity, if no excess pore water pressure is taken into accout. When the excess pore water pressure is allowed for in the stability computation, the value of the seismic coefficient to bring the safety factor detail in the following sections.

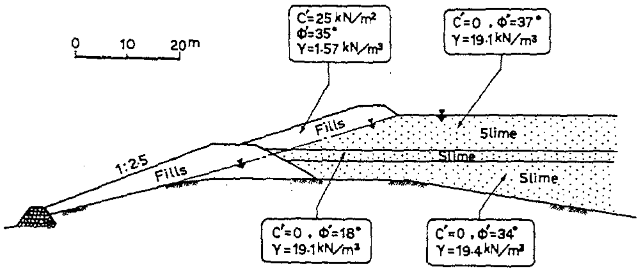

Fig. 20. Cross section of No.2 dike with soil properties used in the stability analysis

down to unity was 0.23.

As described above, the computed factor of safety for No.1 dike becomes equal to unity, if a seismic coefficient of 0.17 is incorporated into the analysis with a proper assessment of excess pore water pressures caused by the earthquake shaking. This magnitude of seismic coefficient was considered reasonable well within the range of 0.15 and 0.25 predicted from the seismic response analysis. It was then sought what the factor of safety would be for the stability of No.2 dike under the identical conditions in which the failure of No.1 dike did occur. Using the seismic coefficient of 0.17 and incorporating the effects of similarly assessed excess pore water pressures, the factor of safety was calculated to be about 1.5 for No.2 dike. The Investigation Committee then concluded that the No.2 dike had been potentially more stable than the embankment of No.1 dam approximately by a factor of 1.5.

POST-EARTHQUAKE STABILITY ANALYSIS

As mentioned in the foregoing, the No.1 dike of the Mochikoshi tailings impoundment pond failed almost at the same time of the major shaking of the main shock and a reasonable interpretation was accorded to the cause of the failure on the basis of the pseudo-static method of stability analysis by incorporating a seismic coefficient and effects of excess pore water pressures generated by the earthquake.

On the other hand, the No.2 dike of the disposal pond survived the damage during the main shock and a series of subsequent shocks as well. However, this dike eventually failed about 24 hours after the main shock while there was no shaking. The cause or mechanism of the failure of this dike was not discussed exhaustively in the report of the Investigation Committee and has been left open to question since then. It is to offer an answer to this question that the present study was undertaken. The basic concepts and procedures for examining the stability of this dike consist in clarifying time-changes in seepage conditions caused by the movement of the phreatic surface within the dike. This aspect of the problem together with procedures for eveluating its effects will be discussed in detail in the following sections.

1. A Method of Analysis for Movement of Phreatic Surface

It is highly likely that the build-up of pore water pressure due to liquefaction in the deposit behind the dike created an unbalanced state of seepage conditions within the deposit underlying the dike. A newly created hydraulic gradient appears to have then raised the elevation of the phreatic surface wihtin the dike, leading eventually to a precarious condition of the embankment even in the static state after a series of earthquake shakings. It would, therefore, be necessary first to explore a possibility of analytical treatment in which time-changes of the phreatic surface can be assessed.

The layout of the present problem in illustrated in Fig. 21. Let it be first assumed that liquefaction due to the main shock of the earthquake

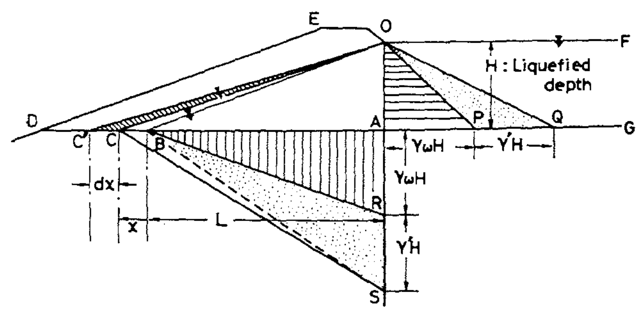

Fig. 21. Setting for analysis of phreatic surface movement

developed to a depth of H and any change in seepage conditions in the deposit below this elevation can be disregarded. The dike constructed of cohesive materials is represented by the section OEDB in Fig. 21 and a deposit of tailings below the dike is represented by a triangular section OBA. It will also be assumed that the phreatic surface had been located, prior to the earthquake, along the interface OB between the main body of the dike and the underlying tailings deposit. If the ground water level within the pond is assumed to coincide approximately with the surface of the tailings deposit, and if the tailings below the dike is assumed to have completed consolidation, then water pressure at depth, H, prior to the earthquake is $\gamma_w H$ and its distribution is hydrostatic as indicated by OAP in Fig. 21, where γ_w is unit weight of water. It may as well be assumed that the pre-earthquake water pressure distribution along a horizontal plane AB at depth, H, is represented by a triangle ABR.

As described in the foregoing section, liquefaction did develop during the shaking of the main shock in the deposit of the disposal pond. However, it is likely that the liquefaction occurred only in the portion of the pond where the tailings deposit is exposed on the surface. The portion of the tailings deposit covered by the dike might not have undergone liquefaction because of a high confining stress exerted by the overlying dike fills. Therefore, it will be assumed that any pore water pressure change in the deposit below the dike were not brought about by the liquefaction of its own but caused by a propagation of the excess pore water pressures from the liquefied deposit behind the dike. Upon development of liquefaction in the pond, the hydrostatic pressure at depth, H, rose by an amount, $\gamma' H$, as indicated by PQ where γ' is unit submerged weight of the tailings material. Therefore, the pressure distribution along the horizontal plane AB may well be assumed to have increased by an amount represented by a triangle RBS in Fig. 21. It may as well be assumed that such a change in pore water pressure distribution has taken place in a relatively short period of time following the onset of liquefaction. The increase in pressure as above then created a hydraulic gradient which is directed towards the surface of the bank and accordingly migration of water is expected to have been motivated in the direction of ascending the phreatic surface within the dike. The configuration of the phreatic surface will be assumed to be a straight line passing through point O at all instances of time during the ascent of the phreatic surface. To develop an analysis for the phreatic surface movement let it be assumed that within a time interval, t, from the onset of liquefaction the phreatic surface has moved from the location OB up to OC, which is represented by the coordinate, x, taken leftwards from point B in Fig. 21. At this instant of time, the hydraulic gradient of water flow may be taken as

$$\frac{\gamma' H}{\gamma_W \ (L + x)}$$

where L is the distance between points A and B in Fig. 21. If the location of the phreatic surface is assumed to move through a small distance, Δx, in a small time interval, Δt, then the amount of water migrating across the current phreatic line OC is calculated on the basis of Darcy law as follows.

$$K\frac{H}{2} \ \frac{\gamma' H}{\gamma_W \ (L + x)} \cdot \Delta t$$

where k is the permeability coefficient and H/2 is an equivalent cross sectional area across which the ground water moves. The water which has migrated across the current phreatic surface is stored in the pores of the soil existing in partially saturated zone. The quantity of water that can be stored is given by

$$\beta \ \frac{H}{2} \ \Delta x$$

where $H\Delta x/2$ indicates an area of the triangle OC'C in Fig. 21 and β is the storage capacity coefficient. Since the amount of inflow must be equal to the quantity of stored water, one obtains

$$\beta \ \frac{dx}{dt} = k \ \frac{\gamma'}{\gamma_W} \ \frac{H}{L + x} \qquad \cdots\cdots\cdot(4)$$

Solving this differential equation under an initial condition x = 0 when t = 0, one obtains

$$\frac{x}{L} = -1 + \sqrt{1 + 2 \ \frac{\gamma'}{\gamma_W} \ \frac{H}{L} \ \frac{kt}{\beta L}} \qquad \cdots\cdots(5)$$

The relationship of Eq.(5) is numerically presented in Fig. 22, where the ratio, x/L, specifying the front of the moving phreatic surface is plotted versus the time factor, $kt/(\beta L)$, for different values of H/L. Considering a most representative case encountered with tailings deposits, the buoyant unit weight, γ', is assumed to be 9.5 kN/m^3.

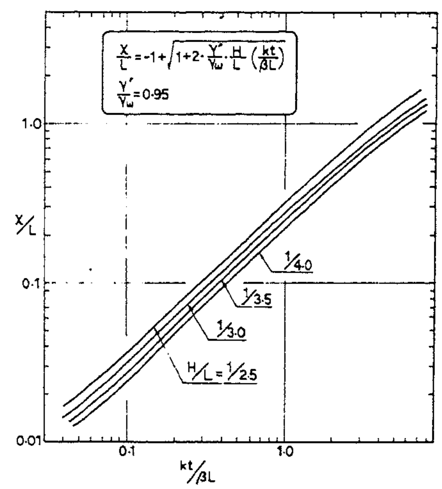

Fig. 22. Travel distance of phreatic surface with time

2. Movement of Phreatic Surface in No.2 Dike

The analysis of liquefaction as described in the preceding section indicated that the deposit in the tailings pond had liquefied during the main shock of the earthquake to a depth of approximately 7 m. It is also known that the phreatic surface through the No.2 dike prior to the earthquake had probably been located at a depth of 3 m from the downslope face of the dike. Therefore, with reference to the geometrical configuration shown in Fig. 23, values of H and L may be set as H = 7 m and L = 21 m, and therefore H/L = 1/3. According to the laboratory tests, permeability coefficient of the dike material was shown to be on the order of $k = 10^{-4}$ cm/sec. With respect to the storage coefficient, β, there is no measured data either from in-situ or from any laboratory test. However, it should be recalled that the storage coefficient is defined as a function of porosity, n, and saturation ratio, Sr, as follows,

$$\beta = n \ (1 - Sr) \qquad \cdots\cdots\cdot(6)$$

The right-hand side of Eq.(6) is equal to the volume of air void per total gross volume of soil. Therefore, if a soil is brought to a completely saturated state as a result of migration of water, the associated storage capacity can be correctly represented by the coefficient given by Eq.(6). However, if the soil

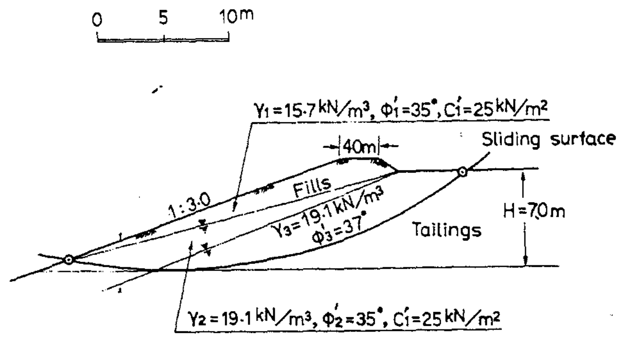

Fig. 23. Sliding surface and soil properties used in the stability analysis

remains still partially saturated, the storage capacity will be somewhat smaller than that predicted by Eq.(6). In spite of some uncertainty as above, Eq.(6) seems to give a value of storage coefficient with a reasonable degree of accuracy that can be used for all practical purposes. For the dike-forming material, the laboratory tests showed that n = 0.6 and Sr = 80 %. Therefore, the value of the storage capacity is calculated through Eq.(6) as being approximately β = 0.12.

The failure of No.2 dike took place around 1:00 p.m. on 15th of January, about 24 hours after the main shock. Therefore, assuming the movement of the phreatic surface to have started following the onset of liquefaction, the period of elapsed time by the occurrence of the failure may be taken as about 24 hours. Then, by introducing t = 24 hours, the time factor in Eq.(5) is calculated as,

$$\frac{kt}{\beta L} = \frac{10^{-4} \times 24 \times 60 \times 60}{0.12 \times 21 \times 100} = 0.034$$

Read off from Fig. 22 a value of x/L corresponding to the time factor of 0.034, one obtains x/L = 0.013 and, therefore, the travel distance of the phreatic surface is estimated to be x = 0.013 x 21 = 0.27 m.

The movement of the phreatic surface as computed above is too short to produce any significant change in a seepage condition influencing the stability of the dike. Therefore, some factors appear to be missing, and some other thoughts may need to be explored.

It is to be recalled here that, in the case of the Izu-Ohshima-Kinkai Earthquake, a series of fairly large aftershocks took place near the dam site beginning around 3:00 a.m. in the morning of 15th of January, 1978 and continued until about 9:00 a.m. on that day. A chain of events that occurred during this period of time is displayed in Fig. 24. It can be seen that a pair of greatest aftershocks with magnitude, 5.8 and 5.4 successively occurred at 7:31 a.m. and 7:36 a.m., respectively, on January 15th, (Tsumura et al, 1978). On the other hand, as mentioned in the foregoing section, a surveillant discovered several strips of fissures running in parallel to the axis of the dike after this series of aftershocks. This fact would appear to indicate that a larger number of invisible

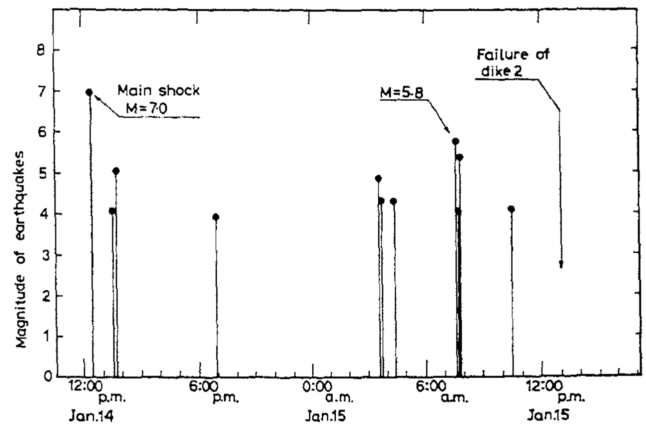

Fig. 24. Occurrence of aftershocks with magnitude greater than 4.0 following the main shock of the Izu-Ohshima-Kinkai earthquake

cracks were created within the fills as a result of the shakings due to the pair of the greatest aftershocks. Therefore, there are reasons to believe that the permeability of the dike had been significantly enhanced. Although there is no way for knowing a correct permeability characteristics, it may well be assumed with a judgement that the gross permeability coefficient had increased to a value on the order of magnitude of k = 2 x 10^{-2}cm/sec as a result of crack development over the slope of the No.2 dike. It may as well be assumed that the period of elapsed time between when the permeability was significantly increased and when the failure took place in No.2 dike is approximately 5.5 hours

With the above reasonings in mind, the time change of the phreatic surface in the No.2 dike may be reevaluated as follows. The time factor, kt/βL, appearing in Eq.(5) can be reevaluated as,

$$\frac{kt}{\beta L} = \frac{2 \times 10^{-2} \times 5.5 \times 60 \times 60}{0.12 \times 21 \times 100} = 1.57$$

With reference to the curve in Fig. 22, the travel distance of the phreatic surface is computed as

$$x = 0.41 \cdot L = 0.41 \times 21 = 8.6 \text{ m}$$

The distance of travel as computed above seems to give a reasonable order of magnitude for the effects of changes in the phreatic surface to be allowed for in evaluating the stability of the slope in No.2 dike.

3. Time Changes in Factor of Safety in No.2 Dike

The simplified analysis for the movement of the phreatic surface as described above indicated that, owing to the development of cracks and consequent drastic increase in permeability of the fills, the phreatic surface must have moved up to a level where the stability of the slope was seriously endangered. Therefore, it will be of interest to investigate how the factor of safety, indicative of the degree of stability, changed with time depending upon the location of the phreatic surface.

The factor of safety was computed by means of the formula in Eq.(3) whereby disregarding the pseudo-static seismic force terms. Exactly the same soil profile and soil strength parameters as shown in Fig. 23 were employed in the stability analyses. The term allowing for the excess pore water pressure was evaluated graphically as illustrated in Fig. 25. This figure shows a state of the dike profile where the front of phreatic surface has advanced to point C halfway between the initial location, B, and the point D at the toe of the slope surface. It is assumed, as mentioned in the foregoing section, that the pore water pressure at point A had increased by an amount, $\gamma' H$, as a result of liquefaction that developed in the pond behind the dike. Therefore, the excess pore water pressure at point A is laid off as the length RS on the diagram by an appropriate scale. Since there exists a sufficient amount of liquefied material behind the dike, and hence a continuous supply of water from behind, the magnitude of excess pore water pressure at point A may be assumed to have remained unchanged for a reasonably long period of time. On the basis of this assumption, the distribution of excess pore water pressure on the horizontal plane ABC may well be represented by a rectangle RSCB. In the computational scheme of stability, a sliding circle was determined from the observed surface of failure in No.2 dike, and the soil mass above this sliding plane was divided into 6 slices as shown in Fig. 25. To illustrate the graphical procedure for estimating the pore water pressure, consider a sliced soil element labelled "4" in Fig. 25. Since the pore water pressure at point I is represented by the length IT and that at the surface point O is zero, the distribution of pore water pressure along the line OI may be approximated by a straight line OT. Therefore, at point H at the bottom center of the slice 4 in question, the total pore water pressure can be determined by drawing a vertical line through point H and locating the point U at its intersection with the line OT representing the distribution of pore water pressure along the line OI. The total pore water pressure at point H is therefore represented by the length HU. The pore water pressures thus determined for all other sliced soil elements, being indicated by upward arrows in Fig. 25, were employed in the computational scheme of stability analysis using the formula in Eq.(3). Factors of safety were computed in this manner for several stages of movement of the phreatic surface. The result of these analyses is presented in Fig. 26. by plotting the computed factor of safety against the travel distance of the phreatic surface. The corresponding period of elapsed time computed through Eq.(5) is also indicated in Fig. 26. In the static condition prior to the earthquake, the factor of safety was computed as being 2.75 as mentioned in the foregoing, but it dropped drastically to 1.85 upon development of liquefaction in the tailings deposit behind the No.2 dike due to the shaking of the main shock which occurred at 12:30 p.m. on January 14, 1978. It is to be noted that at this stage the pore water pressure increase due to the liquefaction is assumed to have propagated into the portion

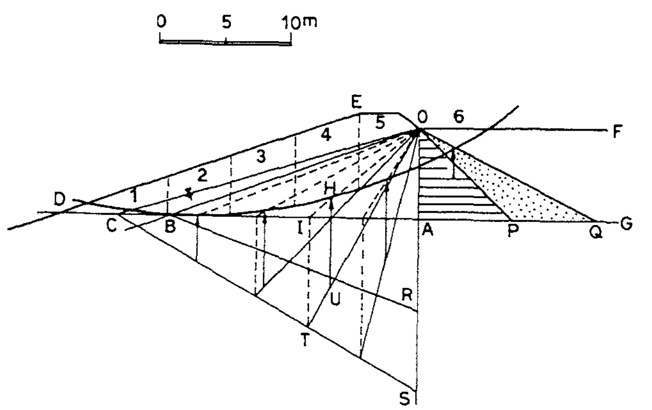

Fig. 25. Layout for the stability analysis

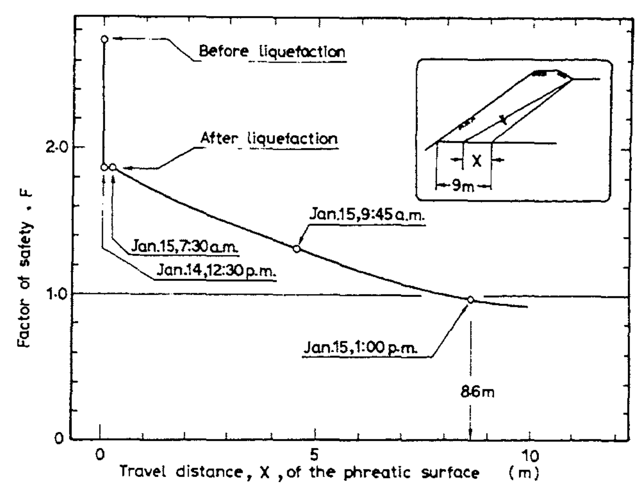

Fig. 26. Change of factor safety caused by the movement of phreatic surface

of the tailings deposit underlying the dike but not yet pushed up the initial level of the phreatic surface prior to the earthquake. In the computational scheme shown in Fig. 25, the distribution of pore water pressure along the horizontal plane GD was taken to be a triangle of ASB for the stability analysis of this stage. Since no singificantly strong aftershock had taken place until 7:30 a.m. in the morning of the next day, the front of the phreatic surface had not presumably advanced to an extent producint any significant change in the computed factor of safety. However, when a couple of large aftershocks occurred around 7:30 a.m., several strips of visible fissures developed over the surface of the dike, leading to a sharp increase in the permeability of the dike fills. From then on, the front of the phreatic surface had presumably moved at a faster rate whereby reducing gradually the factor of safety. The decreasing feature of the computed factor of safety during this stage is also shown in Fig. 26. At about 1:00 p.m., 5.5 hours after the occurrence of the large aftershocks, the phreatic surface had probably moved through a distance of about 8.6 m approaching the toe of the dike surface bringing the embankment to a very precarious state. The computed factor of safety at this stage was 0.98 as accordingly indicated in Fig. 26, and, therefore, the safety of the dike is considered to have been seriously endangered. It is indeed at this stage that the failure actually took place in the fills of the No.2 dike.

Although the reasonings as above can provide a simple interpretation for the mechanism triggering the post-earthquake failure of the dike, they are based on several unverified assumptions. Among the most critical but most difficult to evaluate by any means is the permeability coefficient of the dike-composing fills containing numerous cracks and fissures. The assumption on the distribution of liquefaction induced pore water pressure is also unproved and could be too much of approximation. Therefore, the reasonings as above may have to be taken qualitatively rather than in the quantitative sense.

CONCLUSIONS

About one day after the main shock of the Izu-Ohshima-Kinkai earthquake, a failure occurred in an embankment of No.2 dike enclosing the tailings disposal pond at Mochikoshi, Izu, Japan. To clarify the mechanism triggering the slide, a simple analysis was made for an upward movement of the phreatic surface within the dike which is activated by an excess pore water pressure resulting from liquefaction of the tailings deposit behind the dike. With a proper assessment of permeability of fills in the dike, and based on several assumptions, the analysis result indicated a significant amount of movement of the phreatic surface which could have occurred in the dike during a period of several hours from the time of major aftershocks to the dike failure. For several key instances of time with rising phreatic surface, a series of static slope stability analyses was made using the conventional method whereby allowing for redistribution of excess pore water pressures generated by the earthquake. The factor of safety computed for the stage immediately after the main shock was 1.85 but following a series of aftershocks, the factor of safety was conceived to have decreased gradually due to a sharp increase in permeability of the dike fills caused by the development of cracks and fissures in the embankment. About 5.5 hours after the occurrence of the aftershocks, the computed factor of safety dropped to a value close to unity, indicating that the bank was brought to a very precarious state. The computed result of analysis was thus shown to be coincident with what actually happened in the embankment.

ACKNOWLEDGEMENTS

The investigation of the Mochikoshi tailings dam failure was conducted under the supervision of the Ministry of International Trade and Industry of the Japanese Government. Part of the information concerning the failure of the dikes was offered by the Mochikoshi mining Co. Detailed data on the seismicity of the Izu-Ohshima-Kinkai earthquake were offered by Dr. K. Tsumura of the Meteorological Agency of the Japanese Government. The author wishes to acknowledge the kindnesses of the above person and organizations in providing the most useful information.

REFERENCES

Aguero, G. (1929), "Formacion de Depositos de Relaves en el Mineral del Teniente," Anales del Instituto de Ingenieros de Chile, No.5 pp.164-187.

Dobry, R. and Alvarez, L. (1967), "Seismic Failures of Chilean Tailings Dams," Proc. ASCE, Vol.93, SM 6, pp.237-260.

Investigation Committee (1979), Report on the Incidents of Mochikoshi Tailings Disposal Dams.

Ishihara, K. and Nagao, A. (1983), "Analysis of Landslides during the 1978 Izu-Ohshima-Kinkai Earthquake," Soils and Foundations, Vol.23, No.1, pp.19-37.

Ishihara, K., Toroncoso, J., Kawase, Y. and Takahashi, Y. (1980). "Cyclic Strength Characteristics of Tailings Materials," Soils and Foundations, Vol.20, No.4, pp.127-142.

Ishihara, K., Yasuda, S. and Yokota, K. (1981) "Cyclic Strength of Undisturbed Mine Tailings," Proc. International Conference on Recent Advances in Geotechnical Earthquake Engineering and Soil Dynamics." St. Louis, Vol.1, pp.53-58.

Marcuson, W. F., Ballard, R. F. and Ledbetter, R. H. (1979), "Liquefaction Failure of Tailings Dams Resulting from the Near Izu Ohshima Earthquake, 14 and 15 January, 1978," Proc. 6th Panamerican Conference on Soil Mechanics and Foundation Engineering, Lima, Vol.2, pp. 69-80.

Ohashi, A., Iwasaki, T. and Kawashima, K. (1978), "Estimate of Shaking Intensity during the January 1978 Izu-Ohshima-Kinkai Earthquake Based on Overturning of Tombstones." Report the Public Works Research Institute of Japan, No.1399 (in Japanese)

Okusa, S and Anma, S. (1980), "Slope Failures and Tailings Dam Damage in the 1978 Izu-Ohshima-Kinkai Earthquake," Engineering Geology, Elsevier Scientific Publishing Co. Vol.16, pp.195-224.

Tsumura, K., Karakama, I., Ogino, I. and Takahashi, M. (1978), "Seismic Activities Before and After the Izu-Ohshima-Kinkai Earthquake of 1978," Bulletin of the Earthquake Research Institute, University of Tokyo, Vol.53, pp.675-706. (in Japanese)